November 2001

# Scanning Impedance Microscopy: From Impedance Spectra to Impedance Images

Sergei V. Kalinin
*University of Pennsylvania*

Dawn A. Bonnell
*University of Pennsylvania*, bonnell@lrsm.upenn.edu



Copyright Materials Research Society. Reprinted from MRS Proceedings Volume 699.
2001 Fall Meeting Symposium R
Electrically Based Microstructural Characterization III
Publisher URL:http://www.mrs.org/members/proceedings/fall2001/r/R1_2.pdf

# Scanning Impedance Microscopy: From Impedance Spectra to Impedance Images

**Abstract**
Impedance spectroscopy has long been recognized as one of the major techniques for the characterization of ac transport in materials. The primary limitation of this technique is the lack of spatial resolution that precludes the equivalent circuit elements from being unambiguously associated with individual microstructural features. Here we present a scanning probe microscopy technique for quantitative imaging of ac and dc transport properties of electrically inhomogeneous materials. This technique, referred to as Scanning Impedance Microscopy (SIM), maps the phase and amplitude of local potential with respect to an electric field applied across the sample. Amplitude and phase behavior of individual defects can be correlated with their transport properties. The frequency dependence of the voltage phase shift across an interface yields capacitance and resistance. SIM of single interfaces is demonstrated on a model metal-semiconductor junction. The local interface capacitance and resistance obtained from SIM measurements agrees quantitatively with macroscopic impedance spectroscopy. Superposition of a dc sample bias during SIM probes the *C-V* characteristics of the interface. When combined with Scanning Surface Potential Microscopy (SSPM), which can be used to determine interface *I-V* characteristic, local transport properties are completely determined. SIM and SSPM of polycrystalline materials are demonstrated on $BiFeO_3$ and *p*-doped silicon. An excellent agreement between the properties of a single interface determined by SIM and traditional impedance spectra is demonstrated. Finally, the applicability of this technique for imaging transport behavior in nanoelectronic devices is illustrated with carbon nanotube circuit.

**Comments**

2001 Fall Meeting Symposium R
Electrically Based Microstructural Characterization III
Publisher URL:http://www.mrs.org/members/proceedings/fall2001/r/R1_2.pdf

Mat. Res. Soc. Symp. Proc. Vol. 699 

# Scanning Impedance Microscopy:
# From Impedance Spectra to Impedance Images

Sergei V. Kalinin and Dawn A. Bonnell
Department of Materials Science and Engineering, University of Pennsylvania,
3231 Walnut St, Philadelphia, PA 19104

## ABSTRACT

Impedance spectroscopy has long been recognized as one of the major techniques for the characterization of ac transport in materials. The primary limitation of this technique is the lack of spatial resolution that precludes the equivalent circuit elements from being unambiguously associated with individual microstructural features. Here we present a scanning probe microscopy technique for quantitative imaging of ac and dc transport properties of electrically inhomogeneous materials. This technique, referred to as Scanning Impedance Microscopy (SIM), maps the phase and amplitude of local potential with respect to an electric field applied across the sample. Amplitude and phase behavior of individual defects can be correlated with their transport properties. The frequency dependence of the voltage phase shift across an interface yields capacitance and resistance. SIM of single interfaces is demonstrated on a model metal-semiconductor junction. The local interface capacitance and resistance obtained from SIM measurements agrees quantitatively with macroscopic impedance spectroscopy. Superposition of a dc sample bias during SIM probes the *C-V* characteristics of the interface. When combined with Scanning Surface Potential Microscopy (SSPM), which can be used to determine interface *I-V* characteristic, local transport properties are completely determined. SIM and SSPM of polycrystalline materials are demonstrated on $BiFeO_3$ and *p*-doped silicon. An excellent agreement between the properties of a single interface determined by SIM and traditional impedance spectra is demonstrated. Finally, the applicability of this technique for imaging transport behavior in nanoelectronic devices is illustrated with carbon nanotube circuit.

## INTRODUCTION

Properties and performance of electronic devices are crucially dependent on interface-related phenomena. The most versatile tools for semiconductor characterization are impedance spectroscopy and dc transport measurements. The typical applications of impedance spectroscopy differentiate grain boundary, grain interior and electrode impedances by fitting the impedance data to corresponding equivalent circuit models. This approach addresses the average properties of a polycrystalline material and little or no information is obtained about the properties of the individual elements. Moreover, for complex (e.g. multiphase) systems the equivalent circuits rapidly become complex and non-unique. A number of approaches have been suggested to separate the impedance response of individual structural elements, such as microimpedance spectroscopy using patterned contact arrays[1,2,3] or studies of bicrystal samples.[4,5] However, the correlation of average transport properties with individual microstructural elements requires <u>spatially resolved</u> imaging of dc and ac transport properties. Significant progress has been achieved by measuring quasistatic surface potential distributions in laterally biased samples using both AFM and STM based techniques; however, no SPM technique assessing ac transport behavior existed until now. Scanning Impedance Microscopy is presented as a novel microscopic technique yielding impedance images of complex systems that can be easily correlated with traditional atomic force microscopy (AFM) images or other microscopies (TEM, SEM, optical). The frequency dependent transport behavior is especially critical for systems with high dielectric constants, semiconductors, and nano- and molecular electronic devices.

## RESULTS AND DISCUSSION

Scanning Impedance Microscopy (SIM)[6,7] differs from other probe microscopies in that a modulating electric signal is applied laterally across the surface. In the absence of a probe tip this would be a standard impedance spectroscopy technique. SPM tip acts as a mobile voltage sensor thus giving the advantage of spatial resolution. Due to the relatively large (~10-100 nm) tip surface separation the input impedance of the sensor is almost infinite precluding voltage divider effects. The validity of this approach was verified against a known calibration standard (Schottky metal-semiconductor diode) on which SIM was used to obtain local *C-V* and *I-V* characteristics of the interface. Later SIM was applied to the characterization of complex material systems.

In SIM the tip is held at constant bias $V_{dc}^{tip}$ and a lateral bias $V_{lat} = V_{dc}+V_{ac}\cos(\omega t)$, is applied across the sample. The surface topography is accounted for in a usual fashion. The bias induces oscillations in surface potential $V_{surf} = V_s + V_{ac}(x)\cos(\omega t + \varphi(x))$, where $\varphi(x)$ and $V_{ac}(x)$ are position dependent phase shift and voltage oscillation amplitude and $V_s$ is the dc surface potential. Oscillation in surface potential results in a periodic force acting on the dc biased tip. The lock-in system detects phase and amplitude of tip vibration as shown on Fig. 1. The phase and amplitude of the cantilever oscillation comprise SIM phase and amplitude images at a given frequency. Under some very general assumptions, the phase lag between the surface voltage and cantilever oscillation is constant; therefore, by measuring the phase of the mechanical oscillations of the cantilever position dependent phase angle of voltage oscillations, $\varphi(x)$, is obtained. The relationship between cantilever oscillation amplitude and voltage oscillation amplitude is less straightforward, but can also be explicitly obtained and $V_{ac}(x)$ can be mapped directly. Images can be acquired as a function of frequency from 300 Hz to ~100kHz.

Transport properties of individual interfaces can be reconstructed from voltage phase angle and amplitude. For systems with a single electroactive interface (grain boundary, *p-n* junction, etc), an analytical expression for the phase shift across the interface, $\varphi_d = \varphi_1 - \varphi_2$, and amplitude ratio $\beta = A_2/A_1$, can be obtained as a function of interface capacitance, $C_d$, interface resistance, $R_d$, and resistance of circuit termination, $R$ [Fig. 2].[8] Specifically, in the low frequency limit, $\omega < 1/R_d C_d$ ,voltage phase shift at the interface is determined by interface capacitance and resistance and by the resistance of the current limiting resistor. In the high frequency limit, voltage phase shift is determined by interface capacitance and circuit termination only, $\tan(\varphi_d) = 1/\omega C_d R$. Therefore, SIM phase imaging at frequencies *above* the relaxation frequency of the interface quantifies interface capacitance. Additional information can be obtained from the fine structure of phase and amplitude profiles.

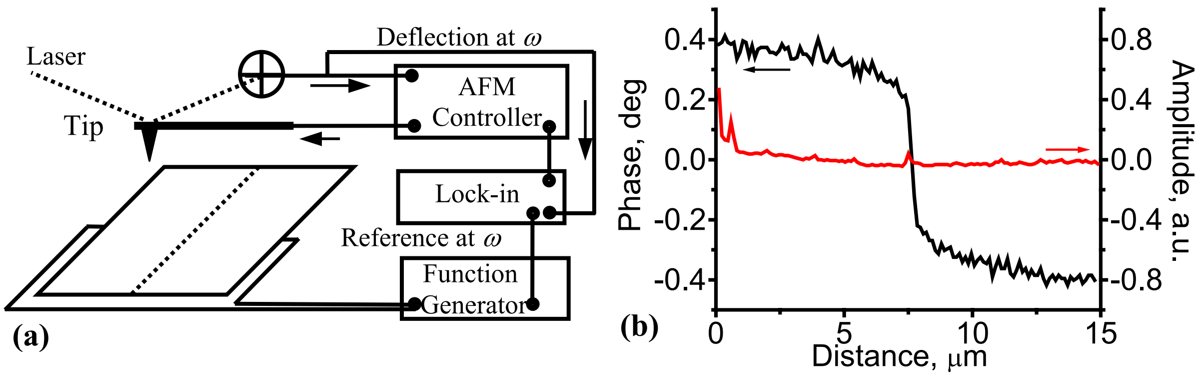


**Fig. 1.** Experimental setup for scanning impedance microscopy (a) and typical phase and amplitude profiles across a grain boundary in $SrTiO_3$ bicrystal in the high frequency regime (b).

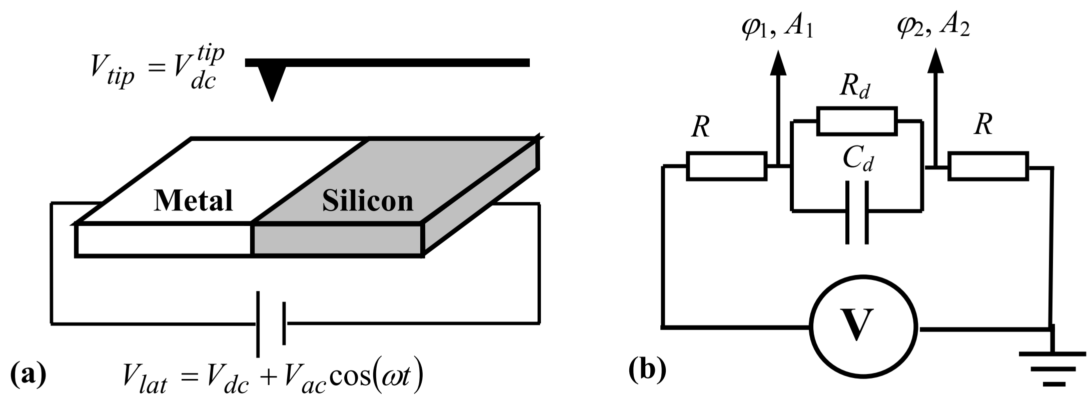


**Fig. 2.** Schematics of scanning impedance microscopy (a) and equivalent circuits for SIM of the single interface (b). $R_d$ and $C_d$ are the (unknown) capacitance and resistance of the interface, $R$ is the circuit termination resistors used in experimental setup. $\varphi_1$, $\varphi_2$, $A_1$ and $A_2$ are the measured phase and amplitude of mechanical cantilever oscillations on the left and right of the interface, from which interface properties can be determined.

Scanning Impedance Microscopy is illustrated on an ideal system: a metal-semiconductor interface (Schottky diode). SIM phase and amplitude images were acquired in the frequency range from 3 to 100 kHz. Shown in Fig. 3 a is the phase profile across the interface for lateral dc biases. In the forward bias region no phase change occurs at the interface, while in the reverse bias region the depletion layer capacitance yields large phase shifts. The absolute cantilever oscillation phase to the left and right of the interface in the reverse bias regime for two different circuit terminations is shown on Fig. 3 b. Note that absolute values of the measured phase is the convolution of tip dynamics (harmonic oscillator; rapid change by 180° at the resonant frequency of the cantilever = 70 kHz) and lateral surface transport. At the same time, $\tan(\phi_d)$ is linear in log-log coordinates with a slope of –1 [Fig. 3 c]. The interface capacitance can be calculated from the intercept and is shown in Table I.

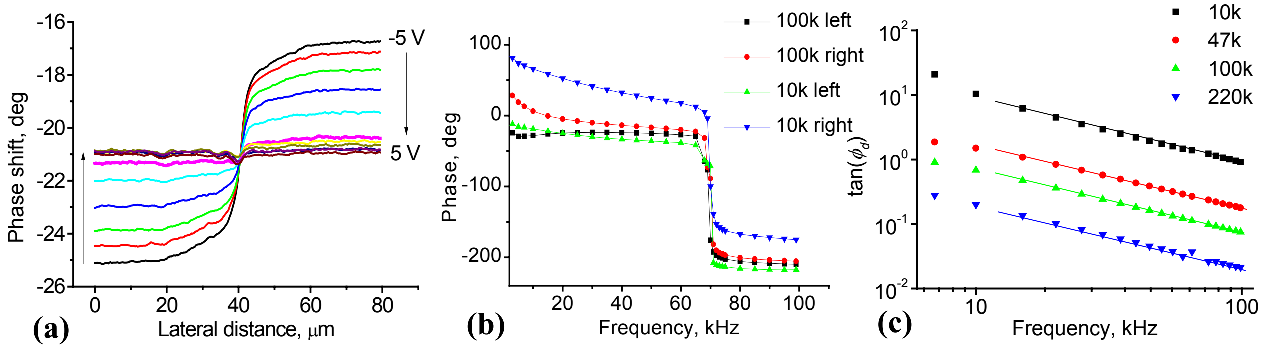


**Fig. 3.** Phase profiles across a metal-semiconductor interface as a function of lateral dc voltage (a), frequency dependence of SIM phase on the left and right of the interface for different circuit terminations (b) and frequency dependence of phase shift of the interface (c).

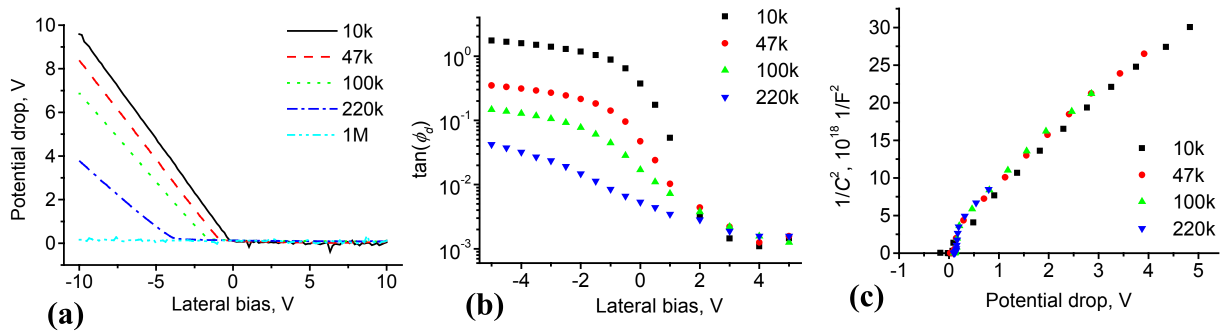


**Fig. 4.** Potential drop at the interface as a function of external bias for different circuit terminations from surface potential measurements (a), SIM phase angle shift at 50 kHz vs. lateral dc bias (b) and interface capacitance vs. potential drop at the interface (c).

Table I.
*Frequency dependence of SIM phase shift*

| R, kOhm | *Intercept* | *Slope* | $C_d$, $10^{-10}$ F | $V_d$, *V for* $V_{dc} = -5$ *V* |
|---|---|---|---|---|
| 10 | 4.94 ± 0.02 | -0.99 ± 0.01 | 1.83 | 4.83 |
| 47 | 4.21 ± 0.01 | -0.98 ± 0.01 | 2.11 | 3.85 |
| 100 | 3.84 ± 0.01 | -0.98 ± 0.01 | 2.32 | 2.86 |
| 220 | 3.29 ± 0.04 | -0.98 ± 0.02 | 3.76 | 0.80 |

The interface capacitance increases for large current limiting resistors *R*. This behavior is due to the fact that for large *R* potential drop at the interface is smaller, therefore the width of depletion region is also smaller and interface capacitance is higher. Thus, by varying the lateral dc bias during SIM imaging the *C*-*V* dependence of the interface can be obtained as shown in Fig. 4. Local potential drop at the interface, $V_d$, is determined as a function of lateral bias, $V_{dc}$, by Scanning Surface Potential Microscopy (SSPM) as shown in Fig. 4 a. Phase angle vs. lateral bias curves differ by more than two orders of magnitude, depending on the circuit termination as shown in Fig. 4 b. Capacitance calculated from phase angle and plotted as a function of potential drop at the interface form a universal linear dependence [Fig. 4 c]. From the *C*-*V* dependence the

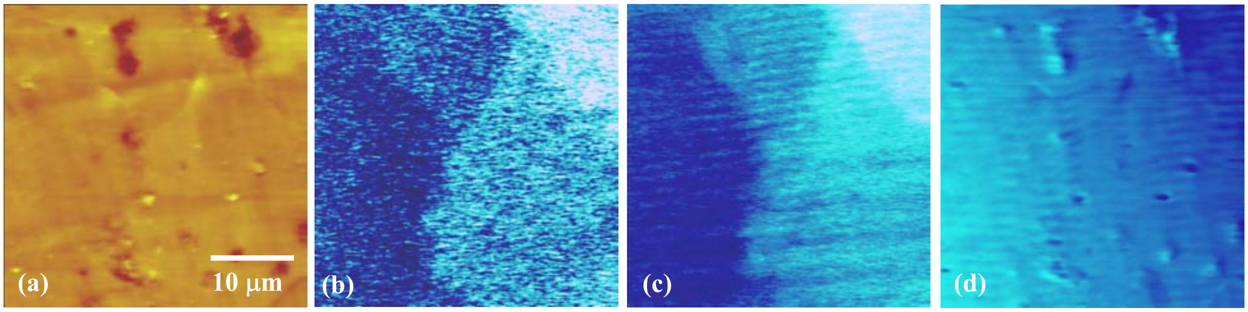

Fig. 5. Surface topography (a), SIM phase image at 10 and 70 kHz (b,c) and SIM amplitude image at 70 kHz for polycrystalline $BiFeO_3$ ceramics. SIM phase images directly visualize capacitive barriers at the interfaces, while amplitude image exhibits uniform ohmic losses within the grains

Schottky barrier height is estimated as 0.6 ± 0.1 eV, as compared to 0.55 eV from conventional *I-V* measurements. Therefore, SIM yields quantitative information on the interface capacitance.

Scanning Impedance Microscopy can be extended to the characterization of complex materials. Shown in Fig. 5 is the surface topography, SIM phase at two different frequencies and SIM amplitude images of polycrystalline $BiFeO_3$. Note that the phase changes abruptly at the interfaces clearly delineating *capacitive* barriers at the grain boundaries. The frequency dependence of interface phase shift across individual grain boundary from SIM measurements can be compared with the value calculated from the impedance spectra demonstrating perfect agreement between the two. The amplitude doesn't change abruptly at the interfaces; rather it exhibits a uniform decrease throughout the sample, indicating ohmic losses within the grains.

SIM was used to image interface behavior in many other systems including $SrTiO_3$ bicrystal grain boundaries, ZnO varistors, grain boundaries in p-doped Si (solar cell) [Fig. 6], Zener diodes, etc.[9] In $SrTiO_3$, the presence of local interface trap states and dielectric behavior in the vicinity of the grain boundary was obtained from SIM data.[10] Shown in Fig. 6 are the surface topography, surface potential and SIM images of *p*-doped Si (solar cell). SIM phase and amplitude images can not be explained by simple *RC* interface approximation, suggesting that SIM addresses fundamental phenomena as minority carrier generation at the grain boundaries. The amplitude doesn't change abruptly at the interfaces; rather it exhibits a uniform decrease throughout the sample, indicating ohmic losses within the grains. SIM can be used to determine local properties in complex materials circuits including carbon nanotubes as illustrated by Fig.7.

## CONCLUSIONS

To summarize, in the present research we developed, and calibrated Scanning Impedance Microscopy. While traditional impedance spectroscopy has poor spatial resolution and existing SPMs are limited by tip-surface interaction and can not assess lateral ac transport properties, SIM combines the advantages of these two approaches. SIM yields local *I-V* and *C-V* characteristics of interfaces with lateral resolution of 50 nm or better. Applicability of SIM extends beyond the semiconductor characterization into the realm of nanoelectronic and molecular electronic devices, e.g. for failure analysis in molecular circuits, etc. These unique possibilities give SIM a special position among SPM techniques and indicate its immense potential for numerous applications. Specifically, SIM allows:

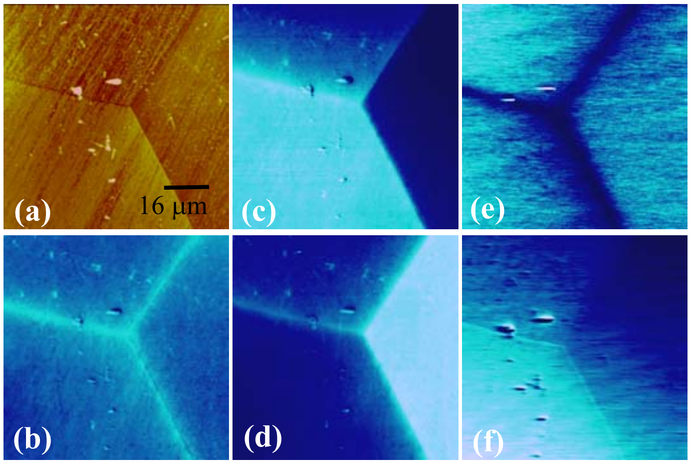


Fig. 6. Topography (a) and surface potential of grounded (b), positively (c) and negatively (d) biased polycrystalline p-doped silicon surface. Positively charged grain boundaries are expected in a *p*-doped material. Application of lateral bias results in the potential drops at the interfaces confirming the high resistivity of grain boundary region. SIM phase (e) and amplitude (f) images of the same region. SIM phase images exhibit complicated structure attributable to minority carrier generation processes in the GB region.

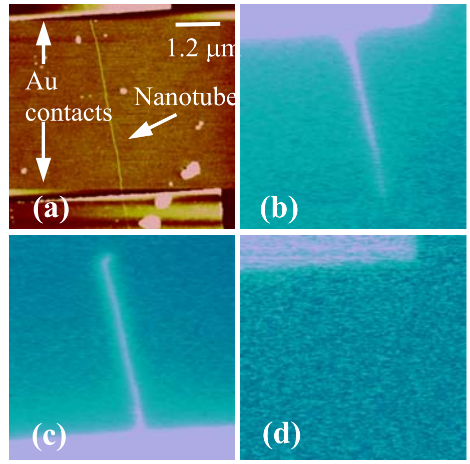


Fig. 7. Topography (a) and SIM amplitude images for an operational (b) and failed (c,d) carbon nanotube circuit. The ac bias is applied to the top electrode (b,d) and bottom electrode (c). Non-uniform decay of voltage amplitude in the operational circuit indicates the regions with different conductivity. In the failed circuit the voltage drop occurs only in the breakdown point.

1. spatially resolved resistance and capacitance measurements of individual interfaces with lateral resolution of ~50 nm or better

2. quantitative determination of frequency and bias dependent interface properties with very high spatial resolution and precision (compared to traditional IS).

3. avoid contact resistances that severely limit the applicability of current sensitive techniques (both microscopic and spectroscopic).

## ACKNOWLEDGEMENTS

We acknowledge the support from MRSEC grant NSF DMR 00-79909 and NSF Grant DMR 00-80863. Authors are grateful to Vladimir Dominko for help with ac and dc transport measurements.

## REFERENCES

[1] J. Fleig, S. Rodewald, and J. Maier, J. Appl. Phys. **87**, 2372-2381 (2000).
[2] S.H. Kim, J.H. Suh, J.G. Park, and Yooho Kim, Jpn. J. Appl. Phys. **39**, 1788-1795 (2000).
[3] A.S. Skapin, J. Jamnik, and S. Pejovnik, Solid State Ionics, **133**, 129-138 (2000).
[4] J.H. Hwang, K.D. Johnson, T.O. Mason, and V.P. Dravid, Appl. Phys. Lett., **76**, 2621-3 (2000).
[5] S. Tanaka and K. Takahashi, J. Eur. Cer. Soc. **19**, 727-730 (1999).
[6] Sergei V. Kalinin and Dawn A. Bonnell, Appl. Phys. Lett. **78**, 1306 (2001).
[7] Dawn A. Bonnell and Sergei V. Kalinin, Scanning Impedance Microscopy of Electroactive Interfaces, patent pending
[8] Sergei V. Kalinin and Dawn A. Bonnell, J. Appl. Phys. **91**, 832 (2002).
[9] www.seas.upenn.edu/~sergei2/research and www.seas.upenn.edu/~bonnell
[10] S.V. Kalinin, D.A. Bonnell, unpublished